Generalised Space-Time Modelling of Rayleigh MIMO channels

David B. Smith and Thushara D. Abhayapala

***Abstract*— A recently proposed space-time model for Rayleigh fading for a multiple-input multiple-output (MIMO) channel with arbitrary spatial separation at the transmitter and the receiver is extended. A space-frequency cross spectrum is derived from a space-time cross correlation for a non-isotropic scatterer distribution around the receiver. A simulation study is performed into the space-time correlation formulation to gain understanding of the changing of some relevant parameters and applying different non-isotropic distributions. The formulations presented can be applied to analyse any numbers of transmit and receive antennas operating in typical time-selective MIMO fading channels, and hence can be used in the design of space-time modems.**

***Index Terms*— Space-time cross correlation, space-frequency cross spectrum, MIMO Rayleigh channels, wireless communications**

I. Introduction

The combination of spatial and temporal diversity are two effective means that can improve communication quality and associated system performance in a rich-scattering wireless environment. The use of multiple-input multiple-output (MIMO) radio channels are a proven means to utilise temporal and spatial diversity. Without designing highly detailed system models, which can be used for individual channel realisations, it is possible to obtain simpler macroscopic system models with a number of possible applications. An important application of these models is a rigorous evaluation of space-time coding schemes, which are understood to be very beneficial for high data-rate systems, both coherent [1] and non-coherent [2]. Other applications have been described in [3], where performance can be parameterised as a function of antenna separation and interleaving depth for designs of space-time modem, or the application described in [4], where models can be used in the design of a two-dimensional pilot-symbol assisted demodulation system.

One such model, used for the purposes of macroscopic system design, based on a Clarke/Jakes model [5], has been proposed in [3] where a rich isotropic distribution of scatterers is assumed around the mobile station (MS), the receiver (Rx). No major scatterers are assumed to be located around the base station (BS), the transmitter (Tx). Space-time correlation and space-frequency cross spectrum functions corresponding to this distribution were derived. This was generalised to the case of a MIMO Rayleigh channel model applicable to many common non-isotropic distribution of scatterers in [6], where the receivers are assumed to be approximately co-located. Previously only a MIMO Rayleigh channel model for a particular non-isotropic distribution had been presented [7].

The results of [6] were extended in [8] to the consideration of spatial separation at the receive antennas. Thus they are applicable to many proposed mobile communication systems with spatial separation at the receive antennas. However the results were limited to the consideration of the space-time correlation. Furthermore it is not recognised throughout [8] that the results are applicable to analysing arbitrary numbers of transmit and receive antennas.

In this paper, a correction is made to the derivation of the space-time cross correlation in [8], and the correlation formulation is further extended to a derivation of the space-frequency cross spectrum. A short simulation study based on the derivations of space-time correlation and space-frequency cross spectrum is also presented giving insight into the changing of relevant parameters to the space-time model, such as Doppler fading parameter, the angle of receiver travel, and angular spread. Different non-isotropic distributions in fast fading channels are also used to give further understanding of the application of the correlation and spectrum functions.

II. Space-Time Cross Correlation Formulation

Consider a MIMO radio channel, with M transmit antennas (Tx) and N_R receive antennas (Rx). Assume that there are no major scatterers around the transmitter antennas , the receiver antennas are immersed in a rich non-isotropic scattering environment. We also assume that the spatial separation between antennas at the transmit and receive side is in azimuth only (2D plane). The derivations in this paper can be applied to either a microcellular or macrocellular time-selective (frequency-nonselective) fading radio scenario. Fig. 1 illustrates the MIMO transmission model between the transmitter and receiver. This model has been previously reported in [6].

With respect to Fig. 1 let us denote the positions of receiver antenna q to be $\boldsymbol{x_q}$ where $\boldsymbol{x_q}$ is a vector from the receiver origin $\mathrm{O_R}$, denoting the centre of the area around which the scatterers are located. The flat fading channel transmission coefficient at time t from Tx antenna p to qth Rx antenna can be written as

$$c_{pq}(t) = \sqrt{\sigma^2} \int A(\hat{\boldsymbol{\alpha}}) \exp\{j2\pi f_D t \hat{\boldsymbol{\xi}}.\hat{\boldsymbol{\alpha}}\} \times \exp\{jk(s_1 + a)\} \exp\{jk\boldsymbol{x_q}\hat{\boldsymbol{\alpha}}\} d\hat{\boldsymbol{\alpha}} \quad (1)$$

D. B. Smith and T. D. Abhayapala are with Wireless Signal Processing National ICT Australia (NICTA), Locked Bag 8001, Canberra, ACT, 2601, (e-mail: David.Smith@nicta.com.au)

T. D. Abhayapala is also with Department of Information Engineering, Research School of Information Sciences and Engineering, the Australian National University, ACT 200, AUSTRALIA (e-mail: Thushara.Abhayapala@anu.edu.au)

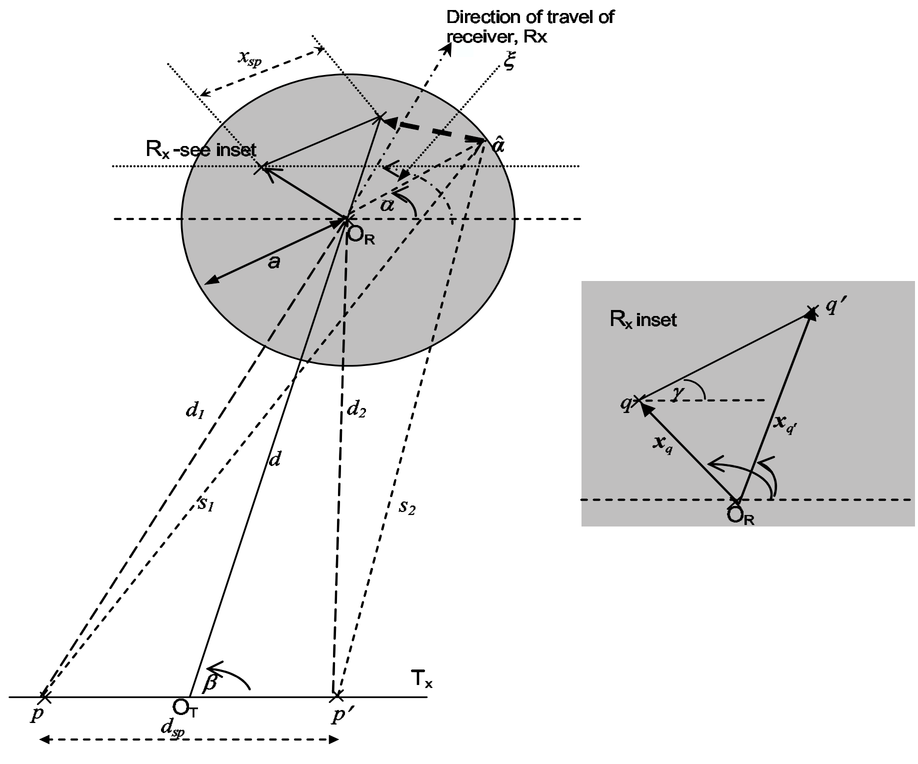

Fig. 1: MIMO Transmission model between transmitter (Tx) and receiver (Rx)

where $\hat{\boldsymbol{\alpha}}$ is a unit vector to represent directions from $\mathrm{O_R}$. $A(\hat{\boldsymbol{\alpha}})$ is the complex scatterer gain at angle $\hat{\boldsymbol{\alpha}}$; σ^2 is the variance of the fading channel, f_D is the maximal Doppler spread caused by the relative motion of the Rx with respect to the Tx, $\hat{\boldsymbol{\xi}}$ is a unit vector in the direction of Rx travel with respect to $\mathrm{O_R}$, a is the uniform distance from $\mathrm{O_R}$ to a non-isotropically distributed scatterer, the wave number $k = 2\pi/\lambda$, where λ represents wavelength, and s_1 is the path length from p at the Tx to a non-isotropically distributed scatterer at a uniform distance from $\mathrm{O_R}$. The subsequent derivation of space-time cross correlation function follows from [8]. The space-time cross correlation at the transmitter and receiver $\rho(d_{sp}, x_{sp}, \tau) \equiv R_{c_{pq}, c_{p'q'}}(d_{sp}, x_{sp}, \tau)$ can be represented as

$$\begin{aligned}\rho(d_{sp}, x_{sp}, \tau) &\equiv E\left\{c_{pq}(t)c^*_{p'q'}(t-\tau)\right\} \\ &= \int P(\hat{\boldsymbol{\alpha}})\exp\{j2\pi f_d t \hat{\boldsymbol{\xi}}.\hat{\boldsymbol{\alpha}}\} \\ &\times \exp\{j\Delta\phi(\hat{\boldsymbol{\alpha}})\}\exp\{jk\{\boldsymbol{x_q} - \boldsymbol{x_{q'}}\}\}\hat{\boldsymbol{\alpha}}.d\hat{\boldsymbol{\alpha}}\end{aligned} \tag{2}$$

where

$$P(\hat{\boldsymbol{\alpha}}) = E\{A|\hat{\boldsymbol{\alpha}}|^2\}. \tag{3}$$

$P(\hat{\boldsymbol{\alpha}})$ is the angular scattering power density distribution, and $\Delta\phi(\hat{\boldsymbol{\alpha}}) = k(s_1 - s_2)$ as in [3], where s_2 is the distance from p' to a non-isotropically distributed scatterer (it should be noted that s_1 and s_2 are functions of $\hat{\boldsymbol{\alpha}}$). In the case that $\hat{\boldsymbol{\alpha}}$=$(1, \alpha)$ then

$$\Delta\phi(\hat{\boldsymbol{\alpha}}) = k[(d_1 - d_2) + z_c\cos\alpha - z_s\sin\alpha] \tag{4}$$

where d_1 and d_2 are the distance from Tx locations p and p' respectively to $\mathrm{O_R}$, and as in [3, App. 1] using far-field assumptions then

$$z_c = c_1\sin\beta, z_s = c_1\cos\beta \tag{5}$$

where $c_1 = d_{sp}\sin\beta \times a/d$, β is the mobile position angle with respect to the end-fire of Tx between $\mathrm{O_T}$ and $\mathrm{O_R}$. If $\boldsymbol{\xi} = (1, \xi)$ and using the far-field assumption in [3, App. 1] that $(d_1 - d_2) = d_{sp}\cos\beta$ then

$$\begin{aligned}&\rho(d_{sp}, x_{sp}, \tau) = \sigma^2\exp(jkd_{sp}\cos\beta) \\ &\times\int_0^{2\pi} P(\alpha)(\exp[j\cos\alpha(2\pi f_D\tau\cos\xi + k(z_c - x_{sp}\cos\gamma))] \\ &\quad\times\exp[j\sin\alpha(2\pi f_D\tau\sin\xi - k(z_s + x_{sp}\sin\gamma))])d\alpha\end{aligned} \tag{6}$$

where $x_{sp} = |\boldsymbol{x_q} - \boldsymbol{x_{q'}}|$, and $\boldsymbol{\gamma} = (1, \gamma), \boldsymbol{\gamma} = \frac{|\boldsymbol{x_q} - \boldsymbol{x_{q'}}|}{\|\boldsymbol{x_q} - \boldsymbol{x_{q'}}\|}$, the unit vector from the qth antenna to the q'th antenna.

We can write the angular power distribution $P(\alpha)$ as, [9],

$$\begin{aligned}P(\alpha) &= \sum_{m=-\infty}^{\infty} C_m\exp(-jm\alpha) \quad \text{where} \\ C_m &= \frac{1}{2\pi}\int_0^{2\pi} P(\alpha)\exp(jm\alpha)d\alpha.\end{aligned} \tag{7}$$

Now we can use (7) in (6), following from the 2-D modal expansion in [10] to give

$$\begin{aligned}\rho(d_{sp}, x_{sp}, \tau) &= \sigma^2\exp(jkd_{sp}\cos\beta)\sum_{m=-\infty}^{\infty} C_m \\ &\times\int_0^{2\pi}\exp(j(-m\alpha + z\sin(\alpha + \psi)))d\alpha\end{aligned} \tag{8}$$

where $\psi = \tan^{-1}\frac{b_1}{a_1}$ and $z = 2\pi\sqrt{a_1^2+b_1^2}$; and as a correction to [8] , $b_1 = f_D\tau\sin\xi - z_s/\lambda - x_{sp}/\lambda\sin\gamma$ and $a_1 = f_D\tau\cos\xi + z_c/\lambda - x_{sp}/\lambda\cos\gamma$.

Now applying the following identity [11],

$$\int_{\psi}^{2\pi+\psi} \exp(j(-m\theta + z\sin\theta))d\theta = 2\pi J_m(z) \tag{9}$$

where $J_m(z)$ is the mth order Bessel function of the first kind, we obtain

$$\rho(d_{sp}, x_{sp}, \tau) = \sigma^2 \exp(jkd_{sp}\cos\beta)2\pi \times \sum_{m=-\infty}^{\infty} C_m \exp(jm\psi)J_m(z). \tag{10}$$

III. Space-Frequency Cross Spectrum Formulation

Following from (10), and in a manner similar to the derivation of the space-frequency cross spectrum in [6], a space-frequency cross spectrum can be found for a non-isotropic distribution of scatterers where there is spatial separation at the receiver in a MIMO radio channel. We first observe that z can be reformulated as

$$z = 2\pi\sqrt{\begin{array}{c}(f_D\tau + (c_2\sin\xi + c_3\cos\xi))^2 \\ +(c_2\cos\xi - c_3\sin\xi)^2\end{array}} \tag{11}$$

where $c_2 = -(z_s + x_{sp}\sin\gamma)$, and $c_3 = (z_c - x_{sp}\cos\gamma)$.

The space-frequency cross spectrum is defined as $S_{c_{pq},c_{p'q'}}(d_{sp}, x_{sp}, f) = \mathcal{F}\{\rho(d_{sp}, x_{sp}, \tau)\}$, where $\mathcal{F}\{\cdot\}$ is the Fourier transform with respect to τ. Therefore

$$S_{c_{pq},c_{p'q'}}(d_{sp}, x_{sp}, \tau) = \sigma^2 \exp(jkd_{sp}\cos\beta) .2\pi \sum_{m=-\infty}^{m=\infty} (C_m.\mathcal{F}\{\exp jm\psi J_m(z)\}) \tag{12}$$

To simplify the above expression, using (11), a result in [11], and the addition theorem for Bessel functions, $\exp(jm\psi)J_m(z)$ can be expressed as

$$\begin{aligned} e^{(jm\psi)}J_m(z) &= \sum_{n=-\infty}^{\infty} j^n J_n(2\pi(f_D\tau + (c_2\sin\xi + c_3\cos\xi))) \\ &\quad \times J_{m+n}(2\pi(c_2\cos\xi - c_3\sin\xi)) \\ &= \sum_{n=-\infty}^{\infty} j^n J_{m+n}(2\pi(c_2\cos\xi - c_3\sin\xi)) \\ &\times \left\{\sum_{m'=-\infty}^{\infty} J_n(2\pi f_D\tau)J_{n-m'}(2\pi(c_2\sin\xi + c_3\cos\xi))\right\}. \end{aligned} \tag{13}$$

Therefore since the space frequency cross-spectrum is defined with respect to τ we need only to find $\mathcal{F}\{J_n(2\pi f_D\tau)\}$ for $n = -\infty \ldots \infty$. Thus following from (12) and (13), $S_{c_{pq},c_{p'q'}}(d_{sp}, x_{sp}, \tau)$ can be expressed as

$$\begin{aligned} S_{c_{pq},c_{p'q'}}(d_{sp}, x_{sp}, f) &= \sigma^2 \exp(jkd_{sp}).2\pi \\ &\times \sum_{m=-\infty}^{\infty}\left\{C_m \sum_{n=-\infty}^{\infty} j^n J_{m+n}(2\pi(c_2\cos\xi - c_3\sin\xi))\right. \\ &\left.\times\left\{\sum_{m'=-\infty}^{\infty}\mathcal{F}\{J_n(2\pi f_D\tau)\}J_{n-m'}(2\pi(c_2\sin\xi + c_3\cos\xi))\right\}\right\} \end{aligned} \tag{14}$$

and using a result from [12, p. 66] and [13, p. 197] we have

$$\begin{aligned} &\mathcal{F}\{J_n(2\pi f_D\tau)\} \\ &= \pm\left(\pi f_D\sqrt{1-\left(\frac{f}{f_D}\right)^2}\right)^{-1} \\ &\quad \times \cos\left(n\sin^{-1}\frac{f}{f_D}\right), \qquad f < f_D \\ &= \mp f_D^n f^{-n}\sin\left(\frac{n\pi}{2}\right)\left(\pi f_D\sqrt{1-\left(\frac{f_D}{f}^2\right)}\right)^{-1} \\ &\quad \times \left(1+\sqrt{1-\left(\frac{f_D}{f}\right)^2}\right)^{-n}, \qquad f > f_D. \end{aligned} \tag{15}$$

The values $\pm x_1 / \mp x_2$ for $n = -\infty \ldots \infty$, depend on whether $n \geq 0$ and/or $|n|$ is even, in which case the transform is $+x_1/-x_2$; otherwise if $n < 0$ and n is odd, one has $-x_1/+x_2$. The term $\mp x_2$ can be disregarded in (15) since we are only considering the frequencies up to the maximal Doppler spread f_D. Thus (14) gives a closed form expression for the space-frequency cross spectrum with a non-isotropic distribution of scatterers.

IV. Simulation of Space-Time Model with Non-Isotropic Distributions

In this section various simulation results will be illustrated for the space-time cross correlation and the space-frequency cross spectrum with non-isotropic scatterer distributions using the results of previous sections. Insight is given into the effects of varying parameters of the correlation and spectrum functions relevant to macroscopic system performance in MIMO flat fading scenarios. These parameters include the Doppler fading parameter, $f_D T_s$ where T_s is the uniform sampling period at the receiver, the angular spread at the receiver defined as the square root of the variance of the particular distribution, and the direction of mobile travel ξ. Further understanding is achieved through applying different non-isotropic distributions, in particular the Von Mises [7] and Laplacian [14] distributions.

In Fig. 2 and Fig. 3 3-D plots are given of the relative magnitude of the cross-correlation function, $|R_{c_{pq},c_{p'q'}}(d_{sp}, x_{sp}, \tau)|$, stated in (10), assuming a Laplacian distribution with an angular spread of 15^o. The radius of scatterers is localised to a distance of 25λ, and the distance d from the BS to the centre of the MS configuration is 1000λ, which approximates a microcellular MIMO radio channel scenario. This is for transmitter spacing d_{sp} from 0.5 to 40λ, x_{sp} from 0 to 5λ; $\xi = 60^o$; $\beta = 30^o$; $\gamma = 45^o$, and AOA of impinging field is 60^o from broadside. In Fig. 2 the Doppler fading parameter $f_D T_s = 0.01$ after $\tau = 20$ received time samples, whereas in Fig. 3 $f_D T_s = 0.05$.

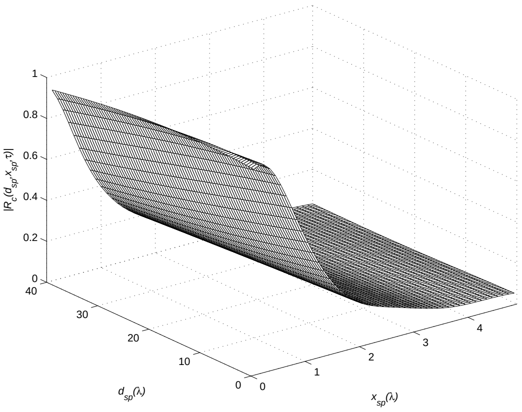

Fig. 2: 3-D plot of magnitude of cross-correlation function $|R_c(d_{sp}, x_{sp}, \tau)|$ for $f_D T_s = 0.01$ after $\tau = 20$ time samples; $\xi = 60^o, \beta = 30^o$ and $\gamma = 45^o$, angular spread = 15^o, for a microcellular MIMO radio channel scenario

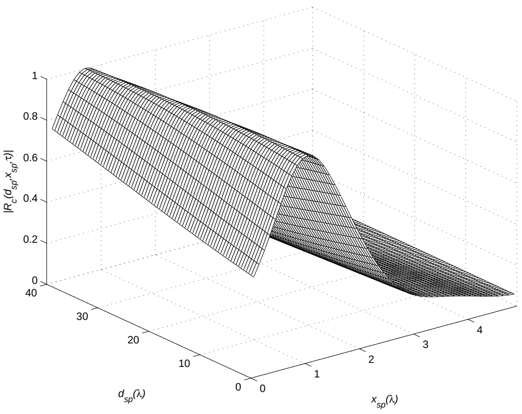

Fig. 3: 3-D plot of magnitude of cross-correlation function $|R_c(d_{sp}, x_{sp}, \tau)|$ for $f_D T_s = 0.05$, all other relevant parameters are the same as Fig. 2

It is clear from both Fig. 2 and Fig. 3 that the dominant influence on the cross-correlation, when comparing the effects of changing the BS spacing, d_{sp}, and the MS spacing, x_{sp}, is x_{sp} for the Laplacian distribution regardless of Doppler fading parameter. In Fig. 4 and Fig. 5 $|R_{c_{pq},c_{p'q'}}(d_{sp}, x_{sp}, \tau)|$ is plotted assuming a Laplacian distribution with an angular spread of 15^o with $d_{sp} = 10\lambda$, varying τ and x_{sp}. As with Fig. 2 and Fig. 3, $f_D T_s = 0.01$ in Fig. 4, and $f_D T_s = 0.05$ in Fig. 5. In Fig. 6 and Fig. 7 all parameters are plotted the same as Fig. 4 and Fig. 5 except a Von Mises distribution is assumed. All other parameters are the same Fig. 2 and Fig. 3.

Fig. 6 and Fig. 7 show similar trends to Fig. 4 and Fig. 5. In comparing both Fig. 4 and Fig. 5, and similarly Fig. 6 and Fig. 7, it is shown that increasing $f_D T_s$ from 0.01 to 0.05 has the effect of shifting where the cross-correlation is maximised, which is intuitive. For the lower Doppler fading parameter,

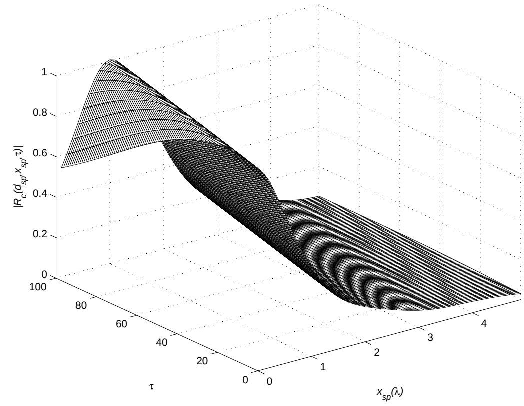

Fig. 4: 3-D plot of magnitude of cross-correlation function $|R_c(d_{sp}, x_{sp}, \tau)|$ for $f_D T_s = 0.01$ assuming a Laplacian distribution with $d_{sp} = 10\lambda$, all other parameters are the same as Fig. 2

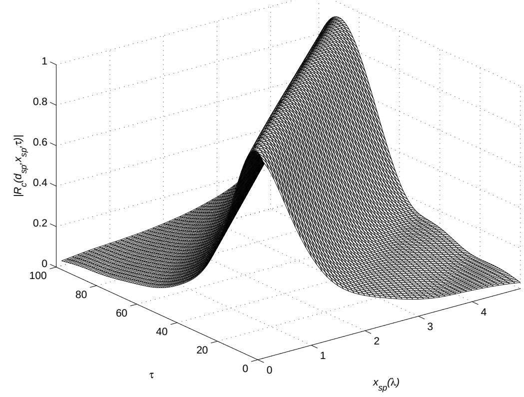

Fig. 5: 3-D plot of $|R_c(d_{sp}, x_{sp}, \tau)|$ for $f_D T_s = 0.05$ and $d_{sp} = 10\lambda$ assuming a Laplacian distribution, all other relevant parameters are the same as Fig. 2

where the fading is less rapid once again the spatial separation at the receiver is dominant in the decrease of the space-time cross correlation. This continued trend is best explained through (10) , $z = \sqrt{a_1^2 + b_1^2}$, a_1 and b_1 are defined for (8), where x_{sp} can be considered to be larger than $f_D\tau$ except where τ is large. From the definition of (8) it is also clear that x_{sp} is considerably larger than $a/d \times d_{sp} \sin\beta$, see (5), for d_{sp} less than 40λ in a MIMO microcellular radio channel scenario, thus explaining it dominating the trend of space-time cross correlation in Fig. 2 and Fig. 3.

In Fig. 8 and Fig. 9, the same parameters are used as Fig. 4 and Fig. 5 with a Laplacian distribution, except that the angular spread is increased from 15^o to 30^o. It can be seen that similar results are obtained as Fig. 4 and Fig. 5. However there is a sharper decrease at smaller antenna separation in the cross-correlation over the range of τ in Fig. 8 when compared with Fig. 4. Also there is a greater diminution of the cross-correlation at higher x_{sp} in Fig. 9 when compared with Fig. 5.

Fig. 10 shows a plot of the space-frequency cross spectrum function, with the same parameters as previous figures assuming a Laplacian distribution at the receiver, an angular

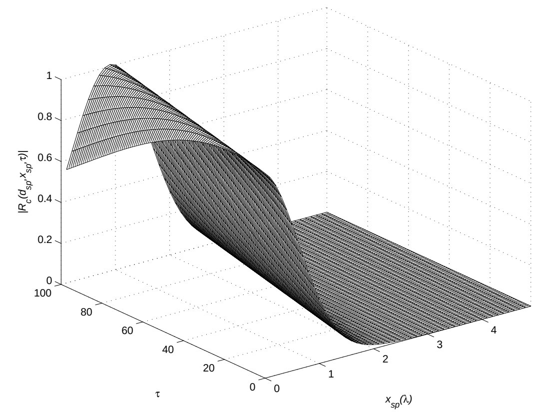

Fig. 6: 3-D plot of magnitude of cross-correlation function $|R_c(d_{sp}, x_{sp}, \tau)|$ for $f_D T_s = 0.01$ assuming a Von Mises distribution with $d_{sp} = 10\lambda$, all other parameters are the same as Fig. 2

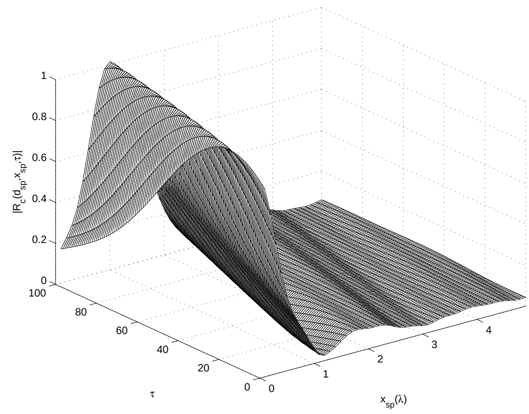

Fig. 8: 3-D plot of magnitude of cross-correlation function $|R_c(d_{sp}, x_{sp}, \tau)|$ for $f_D T_s = 0.01$ assuming a Laplacian distribution with $d_{sp} = 10\lambda$ and angular spread = 30^o, all other parameters are the same as Fig. 2

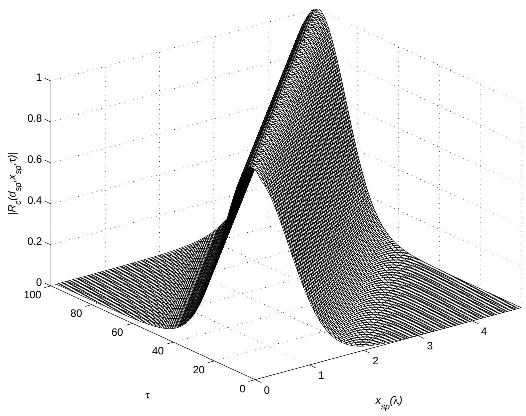

Fig. 7: 3-D plot of $|R_c(d_{sp}, x_{sp}, \tau)|$ for $f_D T_s = 0.05$ assuming a Von Mises distribution with $d_{sp} = 10\lambda$, all other relevant parameters are the same as Fig. 2

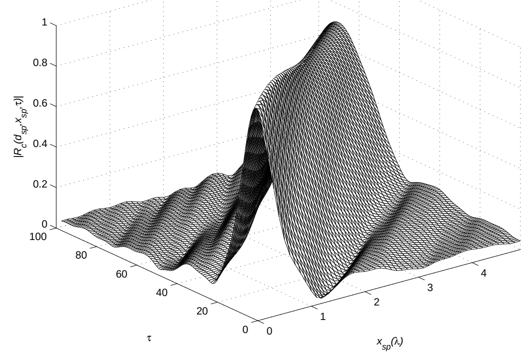

Fig. 9: 3-D plot of $|R_c(d_{sp}, x_{sp}, \tau)|$ for $f_D T_s = 0.05$ and $d_{sp} = 10\lambda$ assuming a Laplacian distribution angular spread = 30^o, all other relevant parameters are the same as Fig. 2

spread of 15^o for two different directions of mobile movement, $\xi = 60^o$ and $\xi = 120^o$, with $x_{sp} = 2\lambda$ and $d_{sp} = 10\lambda$. It is shown in Fig. 10 that a change in the direction of mobile movement has some effect on macroscopic system performance over a range of Doppler frequencies up to the maximal Doppler spread. Both curves are similar to the curve for Doppler frequency spectrum for a single-input single-output (SISO) radio channel with an isotropic distribution (which has the well-known uniform $\cup$ shape).

V. Concluding Remarks

A closed form solution has been found for the space-frequency cross-spectrum which can be applied to continuous fading MIMO channels for time-selective radio scenarios for many common non-isotropic scatterer distributions. The closed form solution can be applied to arbitrary numbers of transmit and receive antennas, and arbitrary transmit and receive antenna spacings, unlike previous derivations for the space-frequency cross spectrum. These solutions can be applied to development of space-time modems and analysis of space-time modulation schemes.

The simulation study of the space-time cross correlation showed the importance of consideration of spatial separation at the receiver due to its dominant effect compared with transmit antenna spacing and also time in the MIMO microcellular radio scenario considered herein. The simulation of the space-frequency cross spectrum illustrated some effect in a change in the direction of receiver travel with respect to the transmitter. It could reasonably be expected that changing other parameters such as angle of receive antennas and mobile position angle would also have effect on the cross spectrum.

The analysis herein could equally be applied to a macro-cellular radio scenario where the scatterer radius and distance is increased proportionally to the values used in analysis in this paper. Furthermore the formulation for space-frequency cross spectrum could be incorporated with a consideration of propagation delay for wideband scenarios to apply the space-frequency cross spectrum formulation herein to continuous time and frequency selective fading radio scenarios.

Acknowledgments

National ICT Australia is funded through the Australian Government's *Backing Australia's Ability* initiative, in part through the Australian Research Council. This research is partially supported by the Australian Research Council grant DP0343804.

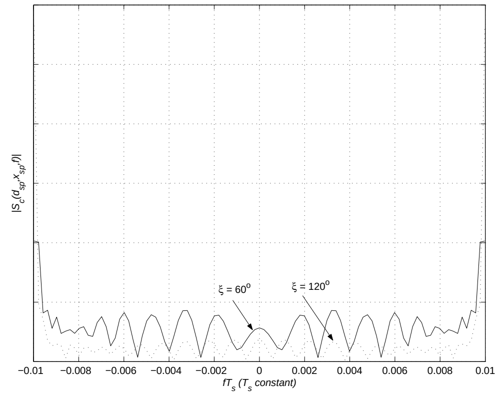

Fig. 10: Plot of $|S_c(d_{sp}, x_{sp}, f)|$ for $f_D T_s = 0.05$ and $d_{sp} = 10\lambda$ assuming a Laplacian distribution with an angular spread = 15^o, all other relevant parameters are the same as Fig. 2

REFERENCES

[1] G. J. Foschini and M. J. Gans, "On limits of wireless communication in a fading environment when using multiple antennas," *Wireless Personal Communications*, vol. 6, no. 3, pp. 311–335, 1998.

[2] L. Zheng and D. N. C. Tse, "Communication on the grassmann manifold: a geometric approach to the non-coherent multiple-antenna channel," *IEEE Trans. Info. Theory*, vol. 48, no. 2, pp. 359–383, Feb.

[3] T. A. Chen, M. P. Fitz, W. Y. Kuo, M. D. Zoltowski, and J. H. Grimm, "A space-time model for frequency nonselective rayleigh fading channels with applications to space-time modems," *IEEE Journal on Selected Areas in Communications*, vol. 18, no. 7, pp. 1175–1190, July 2000.

[4] T-A. Chen, M. P. Fitz, S. Li, and M. D. Zoltowski, "Two-dimensional space-time pilot-symbol assisted demodulation for frequency-nonselective rayleigh fading channels," *IEEE Journal on Selected Areas in Communications*, vol. 52, no. 6, pp. 953–963, June 2004.

[5] W.C. Jakes, *Microwave Mobile Communications*, John Wiley, New York, 1974.

[6] D. B. Smith and T. D. Abhayapala, "Generalised space-time model for rayleigh fading channels with non-isotropic scatterer distribution," *Electronics Letters*, vol. 39, no. 21, pp. 1541–1543, 2003.

[7] A. Abdi, J. A. Barger, and M. Kaveh, "A parametric model for the distribution of the angle of arrival and the associated correlation function and power spectrum at the mobile station," *IEEE Trans. Vehic. Technol.*, vol. 51, no. 2, pp. 425–434, May 2002.

[8] D. B. Smith and T. D. Abhayapala, "On the space-time cross-correlation of a (2,2) MIMO rayleigh channel model," in *Proceedings of the URSI Commission F Triennium Open Symposium*, Cairns, Australia, June 2004.

[9] P. D. Teal, T. D. Abhayapala, and R. A. Kennedy, "Spatial correlation for general distributions of scatterers," *IEEE Sig. Proc. Lett.*, vol. 9, no. 10, pp. 305–308, October 2002.

[10] D. Colton and R. Kress, *Inverse Acoustic and Electromagnetic Scattering Theory*, vol. 93, Springer, New York, 2 edition, 1998.

[11] I. S. Gradshteyn and I. M. Ryzhik, *Tables of integrals, series and products*, Academic Press, London, 6 edition, 2000.

[12] F. Oberhettinger, *Tables of Fourier transforms and fourier transforms of ditributions*, Springer–Verlag, 2 edition, 1990.

[13] L. C. Andrews, *Special functions for engineers and applied mathematicians*, Macimillan, New York, 1985.

[14] K. L. Pedersen, P. E. Mogensen, and B. H. Fleury, "Power azimuth spectrum in outdoor environments," *Electronics Letters*, vol. 33, no. 7, pp. 1583–1584, August 1997.